

Conductivity of doped LaGaO₃ prepared by citrate sol-gel method

I. STIJEPOVIC*, A. J. DARBANDI^{a,b}, V. V. SRDIC

Department of Materials Engineering, Faculty of Technology, University of Novi Sad, Novi Sad, Serbia

^a*Structural Research Division, Technical University Darmstadt, Darmstadt, Germany*

^b*Institute of Nanotechnology, Forschung Zentrum Karlsruhe, Karlsruhe, Germany*

Lanthanum-gallate powders (LSGM), with composition La_{1-x}Sr_xGa_{1-y}Mg_yO_{3-δ} (0 ≤ x, y ≤ 0.2), were prepared using citrate sol-gel method. As-synthesized powders were calcined at 900°C, uniaxially pressed and sintered in air at different temperatures (up to 1450°C). Sintered samples contained cubic perovskite phase, while only pure LaGaO₃ had small amount of the secondary orthorhombic phase. Sintering temperature of 1450°C with dwell time of 2 hours was sufficient to obtain samples with densities higher than 95% TD, with exception of pure LaGaO₃. Impedance spectroscopy measurements confirmed that obtained LSGM ceramics have total conductivity an order of magnitude higher than zirconia-based electrolyte. Thus, citrate sol-gel method used in this work is a promising synthesis route for production of the doped lanthanum-gallate for intermediate temperature solid oxide fuel cells.

(Received March 28, 2010; accepted May 26, 2010)

Keywords: Sol-gel processes, Ionic conductivity, Impedance, Perovskite, LSGM, LaGaO₃

1. Introduction

Oxide-ion conductors have a great role in gas separation processes and in energy conversion devices, such as solid oxide fuel cells (SOFC). At the moment, yttria-stabilized zirconia (YSZ) is generally used in SOFC as an electrolyte and doped LaMnO₃ (LSM) and cermet Ni-YSZ are used as cathode and anode, respectively. However, resistivity of YSZ and LSM become major problem when the temperature is decreased below 800°C, which is considered as a targeted operation temperature of intermediate temperature solid oxide fuel cells (IT-SOFC). One possible candidate to replace YSZ as the electrolyte in IT-SOFC could be Sr and Mg doped LaGaO₃ (LSGM), since it has been reported that it has conductivity of an order of magnitude greater than stabilized zirconia at the same temperature [1, 2, 3, 4]. In this perovskite type material, Sr⁺² and Mg⁺² replace one part of La⁺³ and Ga⁺³ on A and B site, respectively. In this way, oxygen deficient crystal structure is obtained, La_{1-x}Sr_xGa_{1-y}Mg_yO_{3-δ} (0 ≤ x, y ≤ 0.2), and oxygen vacancies are formed to compensate the lack of positive charge.

There are several methods used for synthesis of LSGM, such as solid state route, glycine combustion process, coprecipitation with NH₄OH, Pechini synthesis etc. [3, 4, 5]. All of these have the same problem to obtain single phase material, without any undesired secondary phases, which are generally known to decrease conductivity of LSGM. The second problem is long sintering time needed to achieve densities above 95% TD (in some cases more than 24h). To overcome these obstacles, one should use other, alternative processes such as citrate sol-gel synthesis. Advantages of this LSGM

synthesis are relative simplicity, possibility to synthesize powders with complex compositions and phase purity of sintered ceramics.

In this work, we have investigated conductivity of the series of the LSGM ceramics prepared by citrate sol-gel process. Our goal was to obtain materials with high oxygen-ion conductivity, which could be used as the electrolyte in IT-SOFC.

2. Experimental

The powders were synthesized via citrate sol-gel method, using following starting materials: La(NO₃)₃·6H₂O (Riedel-de Haen), Ga(NO₃)₃·xH₂O (Merck), Sr(NO₃)₂ (Fluka), Mg(NO₃)₂·6H₂O (Merck) and citric acid monohydrate (ZORKAPharma). The value of x in the above formula of gallium nitrate was determined experimentally to be 9 by using thermogravimetric analysis (TGA, BAHR Thermoanalyse STA503).

Stoichiometric amounts of nitrates were dissolved in distilled water to form solutions with cation concentration of 0.2 M. Then, pure citric acid monohydrate was added in molar ratio 2:1 of citric acid to total cations in the solution. The resulting solution was stirred 1h at room temperature and then 1h at 80°C. The solution was then evaporated until a dark yellow resin formed. After overnight drying at 120°C the obtained yellow foam was ground by hand and calcined. The calcination was performed in tube furnace with the heating rate of 1°C/min up to ~270°C, 5°C/min from 270°C to 900°C, and dwell period of 1h at 900°C, followed with furnace cooling. Composition of all powders is represented as La_{1-x}Sr_xGa_{1-y}Mg_yO_{3-δ}, where 0 ≤

$x, y \leq 0.2$ and $\delta = (x+y)/2$. Chemical formulas and notation of sintered samples are given in Table 1.

Table 1. Chemical formulas and composition of prepared LSGM samples.

Chemical formula	Notation
LaGaO ₃	L100G100
La _{0.9} Sr _{0.1} Ga _{0.8} Mg _{0.2} O _{2.85}	L90G80
La _{0.85} Sr _{0.15} Ga _{0.85} Mg _{0.15} O _{2.85}	L85G85
La _{0.85} Sr _{0.15} Ga _{0.8} Mg _{0.2} O _{2.825}	L85G80
La _{0.8} Sr _{0.2} Ga _{0.8} Mg _{0.2} O _{2.8}	L80G80

Calcined powders were uniaxially pressed with the pressure of 625 MPa in steel die to form pellets and then sintered. Temperature regime of sintering had several stages. The heating rate was first 5°C/min and 1h dwell at 500°C, and then 10°C/min up to 1450°C with 2h hold at this temperature, followed with 10°C/min cooling down to the room temperature.

Phase composition of powders and sintered samples were determined by X-ray diffraction method (XRD, Philips PW 1050), using CuK α radiation with $\lambda=0.15406$ nm. Scanning electron microscopy (SEM, JEOL JSM 6460LV) was used to examine the microstructure of sintered samples and to assess their density. Samples were ground and polished and thermally etched at 1300°C for 30 min. Density was also measured by Archimedes method in distilled water. Electrical conductivity measurements were performed by means of impedance spectroscopy (IS, Solartron 1260 Impedance Analyzer) in temperature range from 200°C to 600°C and at frequencies from 0.1 Hz to 1 MHz (perturbation voltage was 30 mV). For this purpose, all measured samples were sputtered with gold to form ~50 nm thick layer on both sides of the pellet. Pt-meshes were used as measuring electrodes. Obtained data was fitted with ZView2 software to calculate resistivity, i.e. conductivity of the LSGM ceramics.

3. Results

Figs. 1 and 2 show the XRD spectra of calcined undoped and doped L90G80 powders respectively. In the undoped LaGaO₃ only cubic phase was identified, but closer examination of XRD pattern (inlet in Fig. 1.) shows peaks with characteristic splitting, which indicates presence of orthorhombic phase too.

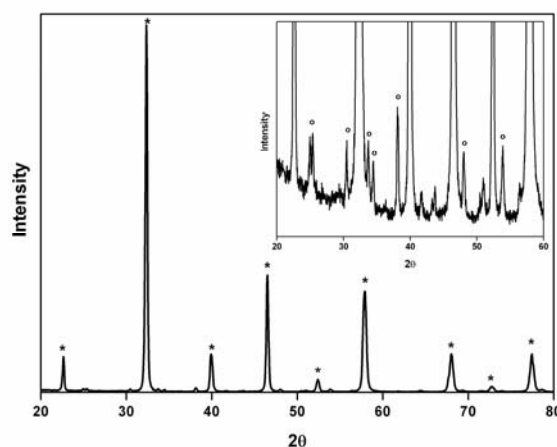


Fig. 1. XRD spectra of the calcined undoped LaGaO₃ powder (inlet: low intensity peaks of the same spectra). (*) represent cubic perovskite phase and (o) represent orthorhombic phase.

In case of the doped powders, the presence of secondary phases is even more pronounced because, beside cubic perovskite phase, they consist also of several other phases, mainly SrLaGa₃O₇ and La₄Ga₂O₉ (Fig. 2).

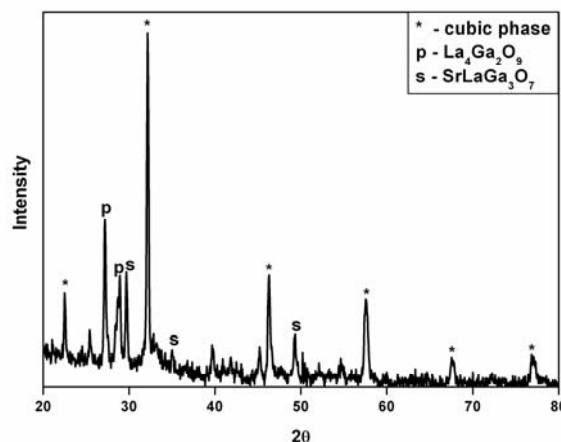


Fig. 2. XRD spectra of the calcined doped L90G80 powder.

After sintering at 1450°C for 2h the cubic perovskite phase is identified, as it can be seen in Figs. 3 and 4. Small amount of orthorhombic phase remained in the undoped sample, in contrast with the doped samples, where secondary phases seem to dissolve or they are present in amount undetectable by XRD. However, at lower sintering temperature (1350°C), even after addition of Sr and Mg, some weak peaks of possible secondary phases have been observed (Fig. 5).

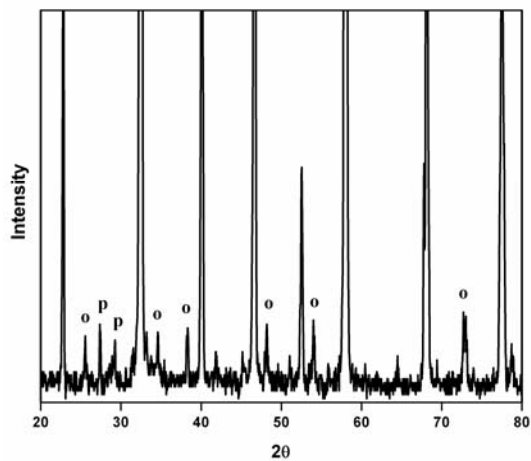


Fig. 3. XRD spectra of the undoped L10G100 sample after sintering at 1450°C for 2h. (o) is orthorhombic phase and (p) is $\text{La}_4\text{Ga}_2\text{O}_9$.

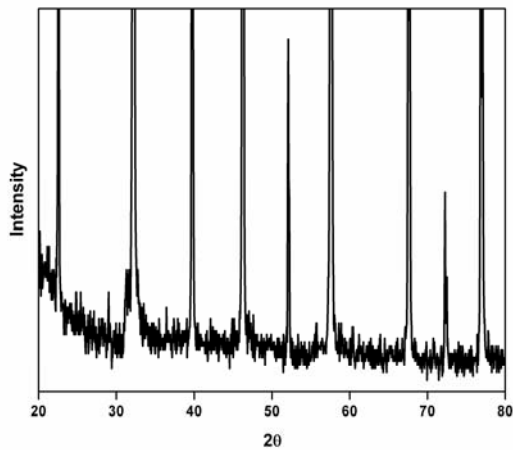


Fig. 4. Low intensity region of XRD spectra of the doped L80G80 sample after sintering at 1450°C for 2h, showing only cubic phase present in the sample.

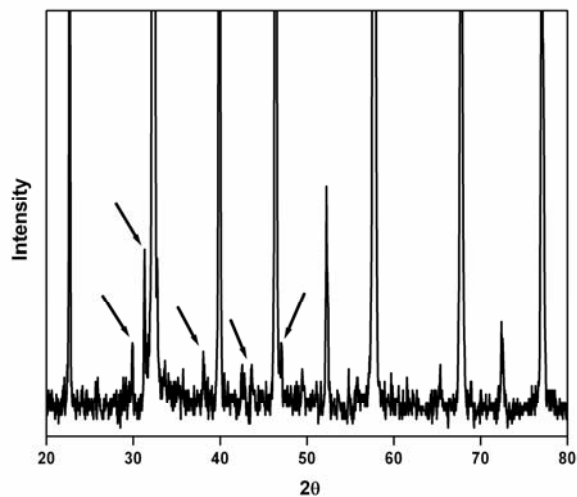
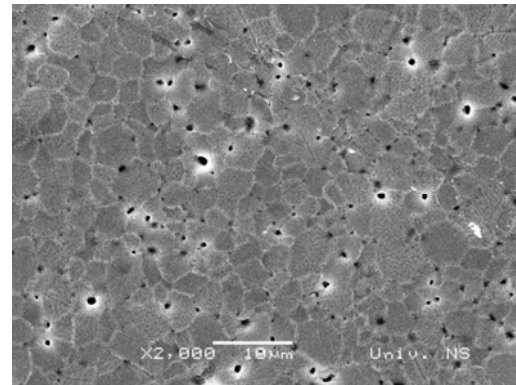
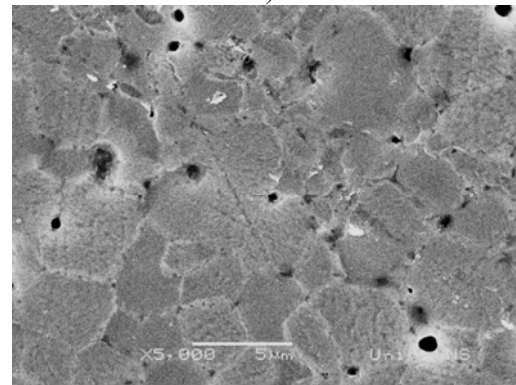


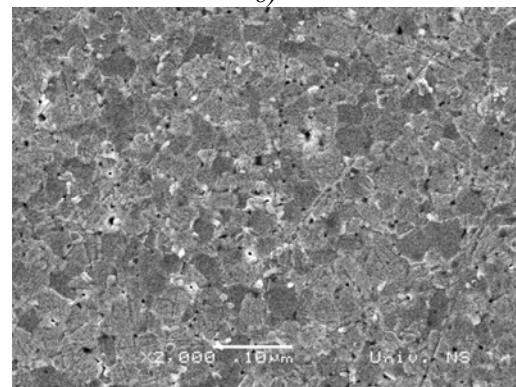
Fig. 5. XRD spectra of the doped L80G80 after sintering at 1350°C for 2h (peaks shown with arrows indicate presence of some secondary phase).



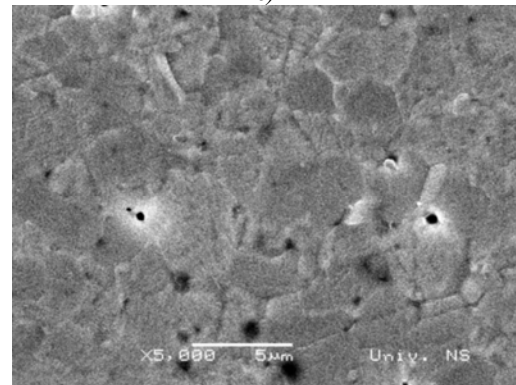
a)



b)



c)



d)

Fig. 6. SEM micrographs of the doped L90G80 (a, b) and L80G80 (c, d) after sintering at 1450°C for 2h under different magnifications.

The microstructure of the sintered pellets was examined with SEM and micrographs have been shown in Fig. 6. In these pictures it could be seen that average grain size is similar in different samples. Also, very few closed pores remained after sintering, and this resulted in high

density values, which were determined by Archimedes method to be >95% TD. Only the undoped LaGaO₃ had density lower than 95% TD, i.e. 93.2% TD.

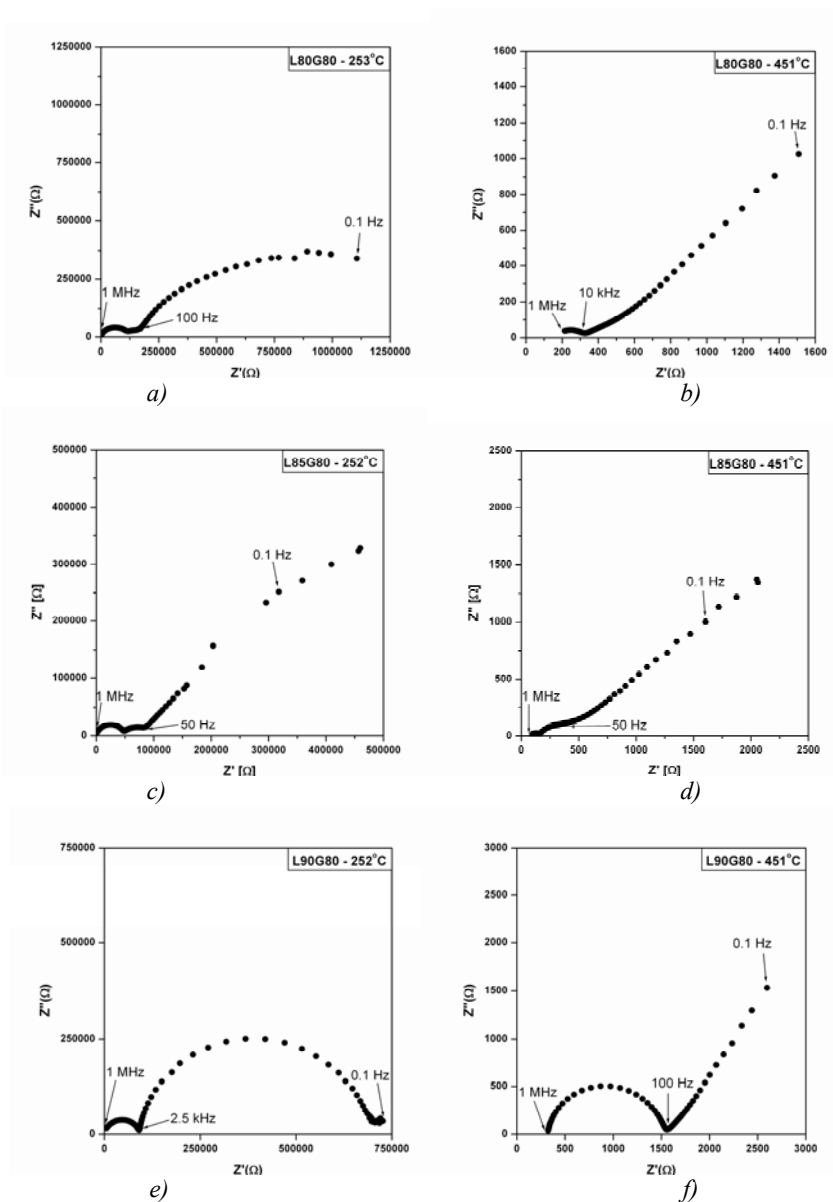


Fig. 7. Several IS spectra of the doped samples: L80G80 (a, b), L85G80 (c, d) and L90G80 (e, f) at different temperatures.

Conductivity measurements were performed by means of ac impedance spectroscopy (IS) on samples L90G80, L85G90 and L80G80. Some results are shown in Fig. 7. For the data fitting we used ZView2 software and the equivalent circuits shown in Fig. 8.

High frequency semicircle represents bulk impedance, intermediate frequency region corresponds to grain boundary resistivity and low frequency spike is consequence of electrode-LSGM interface [10].

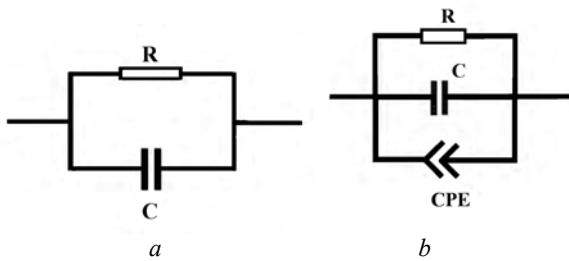


Fig. 8. Equivalent circuits used for fitting: a) parallel R-C circuit and b) parallel R-C-CPE circuit.

Arrhenius plots of bulk, grain boundary and total conductivity, as $\ln(\sigma T)$ against $10000/T$, are shown in Fig. 9 for sample L85G80. Total conductivity at 600°C is approximately $\sim 0.01 \text{ S}\cdot\text{cm}^{-1}$, which is considered as targeted value for the electrolyte in IT-SOFC [14]. Table 2 gives calculated activation energies (E_a) for bulk and grain boundary conductivities, which correspond well with reported values for oxygen ion conductivity in LSGM ceramics [10, 15].

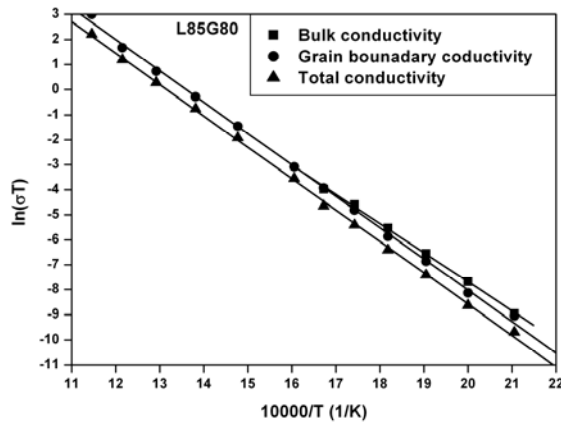


Fig. 9. Arrhenius plot of conductivity for the L85G80.

Table 2. Calculated values of activation energies for all three measured samples

Sample notation	E_a [eV]	
	Bulk	Grain boundary
L80G80	1.0361	1.1123
L85G80	1.0037	1.0795
L90G80	0.974	1.0845

The influence of dopant levels could be revealed from Fig. 10, where total conductivities of the L80G80, L85G80 and L90G80 are shown. All three samples of LSGM have an order of magnitude higher conductivity than zirconia-based electrolytes [16, 17], in the measuring temperature range. Fig. 11 shows bulk (a) and grain boundary (b) conductivities for all three samples.

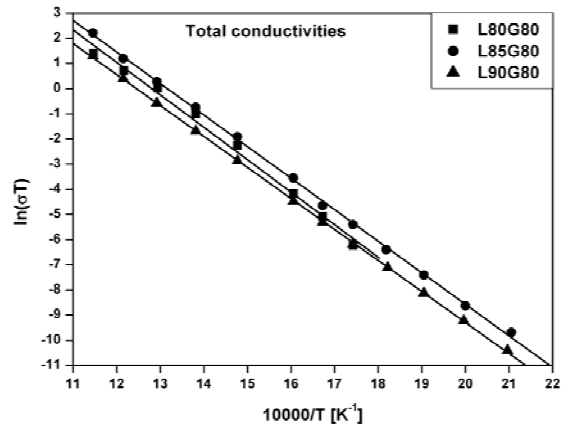
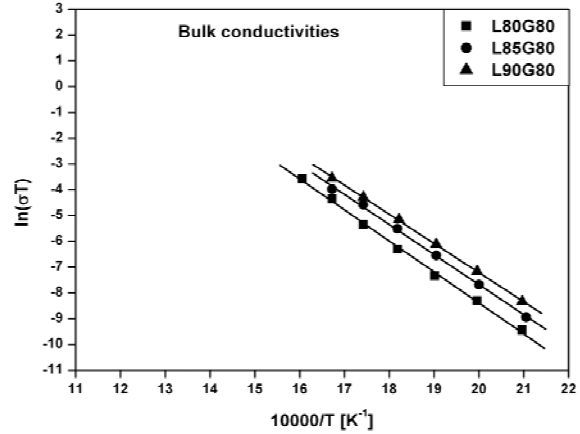
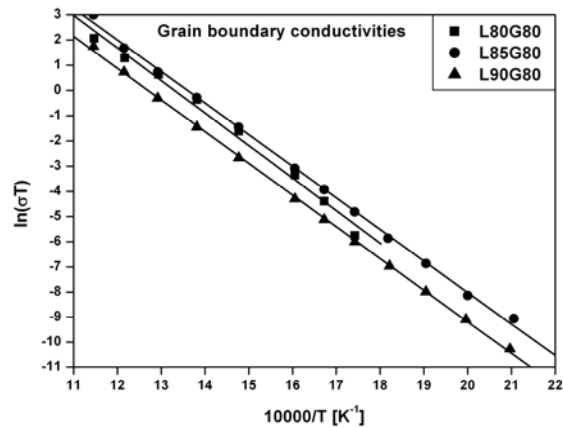


Fig. 10. Total conductivities of all three measured doped samples.



a)



b)

Fig. 11. Bulk (a) and grain boundary (b) conductivities of all three measured doped samples.

4. Discussion

Results shown in Figs. 1 and 2 indicate that after calcination at 900°C for 1 hour various types of undesired phases are still present in doped powders. These phases are commonly formed in all types of synthesis (e.g. solid state, combustion synthesis, spray pyrolysis etc.) [3, 6] and the synthesis of a pure single phase material is rather difficult [3, 4, 7]. It was reported [5, 6, 7] in some previous papers that it is necessary to heat up as-synthesized powders via solid state route and combustion synthesis up to 1500°C to obtain pure LSGM powders. Their explanation was that these secondary phases were thermodynamically stable at temperatures up to 1400°C and that solution would be calcination of powders at higher temperatures. Nevertheless, our main goal in calcination was not to obtain pure crystal LSGM powder but to decompose organic residues, which remained after synthesis, and formation of crystalline particles.

For complete dissolution of secondary phases present in calcined powders, the sintering temperature of 1450°C (2h) is necessary. Also, we could say that doping of LaGaO₃ with Sr and Mg and sintering above 1400°C completely stabilizes cubic crystal structure, which is in good agreement with earlier reported paper [8]. In this research, authors concluded that the cubic form of LaGaO₃ is only stable above 1400°C, with addition of Sr and Mg ions in *A* and *B* sites respectively.

The usage of such high temperature as 1450°C has one more justification if look at microstructure and densities of the sintered samples (Fig. 6). Considering that this was the case of pressureless sintering in air and that dwell time was only two hours, obtained high density values are significant feature of citric acid process used in this work. Other methods for preparation of LSGM ceramics have major problems to obtain densities above 95% TD. This is one important obstacle for standard solid state route, where several heating cycles, at temperatures as high as 1500°C, are needed for density to be greater than 95% [6]. Even with other types of wet chemical processes, like coprecipitation and Pechini synthesis [3, 6, 9] the sample density represents a problem, beside phase purity.

Results of functional characterisation are shown in Fig. 7 as IS spectra which were fitted by two models represented as equivalent circuits in Fig. 8. The first proposed equivalent circuit (Fig. 8a) did not produce any valuable fitting because all semicircles were little bit depressed and the fitting error was high. This parallel *RC* circuit is very often used in IS analysis for ion conducting materials [11, 12], and represents ideal case of ionic conductivity where IS spectra are perfect semicircles. When IS spectra consists of several depressed semicircles [13] constant phase element is added, parallel with *R* and *C*. This behaviour is very common with LSGM ceramics and this is why the second circuit (Fig. 8b) gave much better results (parallel resistor, capacitor and constant phase element), with the smallest errors for *R_b* and *R_{gb}*. Thus, we could say that this is an optimal mathematical

model to fit IS data of LSGM ceramics in this work, which is in a good agreement with some previous reports in literature [11]. Beside that well-known feature of doped LaGaO₃ to produce non-ideal semicircles in IS spectra, another explanation for depressed semicircles could be that even with densities above 95% TD, some pores evidently exist and represent obstacles for ion diffusion process. Also, at this phase of research, we do not exclude possibility that some undesired secondary phases are present in sintered samples and having role as insulators. The amount of these secondary phases was undetectable by XRD but on SEM images (Figs. 6c and 6d) there were some indications that undesired phases probably had been formed at the grain boundary. However, even with this proposed equivalent circuit (Fig. 8b), some problems emerged in fitting data and calculating *C_b* and *C_{gb}* at higher measuring temperatures, e.g. 550 and 600°C. This is due to a narrow frequency range (just up to 1 MHz), which consequently led to a disappearance of a part of semicircles and inability to determine the real values of *C_b* and *C_{gb}*. Nevertheless, the error of fitting for *R_b* and *R_{gb}*, even at those higher temperatures, stayed sufficiently small (<5%) so that we can use these results to calculate conductivity of LSGM ceramics.

The L85G80 sample has the highest total conductivity and this could be explained by the maximum solubility of Sr in the crystal lattice, which is close to 0.16 [7]. Obviously, excess amount of Sr in the L80G80, comparing with L85G80, did not increase number of oxygen vacancies as it had been expected. It seems like redundant Sr has been incorporated along grain boundary, causing decrease in the σ_{gb} of L80G80 (Fig. 11b). Also, it should be noted that increased amount of Sr led to decrease in σ_b (Fig. 11a). This indicates that majority of O²⁻ vacancies have been formed at the grain boundary. This is probably due to the presence of the large number of defects in this region and its high energy state, which enabled lowering of activation energy for vacancy formation.

5. Conclusions

Doped lanthanum-gallates (La_{1-x}Sr_xGa_{1-y}Mg_yO_{3-δ}) were prepared via citrate sol-gel synthesis and air sintered at different temperatures for 2h. After sintering at 1450°C all samples doped with Sr and Mg had densities above 95% TD and cubic perovskite structure in contrast with the pure, undoped samples. Impedance measurements showed that LSGM ceramics possess conductivity almost an order of magnitude higher than commercial yttria stabilized zirconia. Sr-doping higher than *x*=0.15 does not improve the conductivity of LSGM electrolyte and the highest total conductivity of La_{0.85}Sr_{0.15}Ga_{0.8}Mg_{0.2}O_{3-δ} ceramic could be explained by the maximum solubility of Sr in the perovskite lattice, which is close to this level (*x*=0.16). Thus, citrate sol-gel method enabled obtaining LSGM ceramics for IT-SOFC application via low-temperature calcination and short-time sintering.

Acknowledgement

The research was supported by the Serbian Ministry of Science and Technological Development, under the Project "Synthesis of nanopowders and processing of ceramics and nanocomposites for application in novel technologies", No. 142059 and COST 539 Project ELENA.

References

- [1] T. Ishihara, H. Matsuda, Y. Takita, *J. Am. Chem. Soc.* **116** 3801 (1994).
- [2] K. Huang, J. Wan, J. B. Goodenough, *Journal of Materials Science*, **36**, 1093 (2001).
- [3] R. Polini, A. Pamio, E. Traversa, *J. Eur. Ceram. Soc.* **24**, 1365 (2004).
- [4] M. Shi, Y. Xu, A. Liu, N. Liu, C. Wang, P. Majewski, F. Aldinger, *Materials Chemistry and Physics* **114**, 43 (2009).
- [5] A. C. Tas, P. J. Majewski, F. Aldinger, *J. Am. Ceram. Soc.*, **83**(12), 2954 (2000).
- [6] P. Majewski, M. Rozumek, C.A. Tas, F. Aldinger, *J. Electroceram.*, **8**, 65 (2002).
- [7] V. P. Gorelov, D. J. Bronin, Ju. V. Sokolova, H. Nafe, F. Aldinger, *J. Eur. Ceram. Soc.* **21**, 2311 (2001).
- [8] M. Rozumek, P. Majewski, L. Sauter, F. Aldinger, *J. Am. Ceram. Soc.*, **86**(11), 1940 (2003).
- [9] N. S. Chae, K. S. Park, Y. S. Yoon, J. S. Yoo, J. S. Kim, H. H. Yoon, *Colloids and Surfaces A: Physicochem. Eng. Aspects*, **313-314**, 154 (2008).
- [10] M. Kurumada, H. Hara, F. Munakata, E. Iguchi, *Solid State Ionics*, **176**, 245 (2005).
- [11] E. J. Abram, D.C. Sinclair, A.R. West, *J. Electroceram.*, **10**, 165 (2003).
- [12] C. Li, Y. Xie, C. Li, G. Yang, *Journal of Power Sources*, **184**, 370 (2008).
- [13] K. Huang, R.S. Tichy, and J. B. Goodenough, *J. Am. Ceram. Soc.*, **81**(10), 2576 (1998).
- [14] B. C. H. Steele, *J. Mater. Sci.*, **36**, 1053 (2001).
- [15] F. Maglia, U. Anselmi-Tamburini, G. Chiodelli, H. E. Çamurlu, M. Dapiaggi, Z.A. Munir, *Solid State Ionics*, **180** 36 (2009).
- [16] S. P. S. Badwal, K. Foger, *Ceram. Intern.* **22**, 257 (1996).
- [17] P. Mondal, A. Klein, W. Jaegermann, H. Hahn, *Solid State Ionics*, **118**(3-4), 331 (1999).

*Corresponding author: ivan.stijepovic@gmail.com